An iron-57 and tin-119 Mössbauer spectral study of $NdMn_{6-x}Fe_xSn_6$

2005 J. Phys.: Condens. Matter 17 4665

(http://iopscience.iop.org/0953-8984/17/29/009)

INSTITUTE OF PHYSICS PUBLISHING JOURNAL OF PHYSICS: CONDENSED MATTER

J. Phys.: Condens. Matter **17** (2005) 4665–4686 doi:10.1088/0953-8984/17/29/009

An iron-57 and tin-119 Mössbauer spectral study of $NdMn_{6-x}Fe_xSn_6$

Fernande Grandjean[1], Gary J Long[2], Bernard Mahieu[3], J Han[4] and W J James[4]

[1] Department of Physics, B5, University of Liège, B-4000 Sart-Tilman, Belgium
[2] Department of Chemistry, University of Missouri-Rolla, Rolla, MO 65409-010, USA
[3] Department of Chemistry, CSTR, Université Catholique de Louvain, Place L Pasteur, 1, B-1348 Louvain-la-Neuve, Belgium
[4] Department of Chemistry and the Graduate Center for Materials Research, University of Missouri-Rolla, Rolla, MO 65409-010, USA

Received 20 May 2005, in final form 14 June 2005
Published 8 July 2005
Online at stacks.iop.org/JPhysCM/17/4665

Abstract

The iron-57 Mössbauer spectra of the $NdMn_{6-x}Fe_xSn_6$ compounds with $x = 0.5$, 1.0, 1.5 and 2.0 have been obtained at 4.2, 78 and 295 K, and the tin-119 Mössbauer spectra of the $NdMn_{6-x}Fe_xSn_6$ compounds with $x = 0.0$, 0.5, 1.0, 1.5 and 2.0 have been obtained between 85 and 370 K. A successful and rational analysis of the spectra is based upon a Wigner–Seitz cell analysis of the $HoFe_6Sn_6$-structure with the $Immm$ space group for $NdMn_6Sn_6$ and of the $TbFe_6Sn_6$-structure with the $Cmcm$ space group for the $NdMn_{6-x}Fe_xSn_6$ compounds with $x = 0.5$, 1.0, 1.5 and 2.0. Both the iron-57 and the tin-119 spectra reveal that the spin reorientation exhibited by these compounds at low temperature is extremely sensitive to the cooling rate of the samples. Specifically, samples that are slowly cooled from 295 to 78 K retain their 295 K magnetic structure and do not exhibit a spin reorientation. In contrast, samples that are quenched from 295 to 78 K and then further cooled to 4.2 K exhibit a spin reorientation. The ca 15 T iron-57 hyperfine fields observed at 4.2 K are unusually small, whereas the ca 25 T tin-119 transferred hyperfine fields observed at 85 K are unusually large. These latter large fields, as well as the improvement in Curie temperature and magnetization with increasing iron content in the $NdMn_{6-x}Fe_xSn_6$ compounds, are discussed in terms of earlier electronic structure calculations.

1. Introduction

The RT_6Sn_6 compounds, where R is Mg, Sc, Y, Zr, Hf or a rare-earth element and T is Fe or Mn, crystallize in three different space groups with a wide variety of magnetic structures [1–5]. More specifically, $NdMn_6Sn_6$, YFe_6Sn_6 and $HoFe_6Sn_6$ crystallize in the $Immm$, number 71, space group, the RFe_6Sn_6 compounds, where R is Gd, Tb, Dy or Er, crystallize in the $Cmcm$,

number 63, space group and the RFe_6Sn_6 compounds, where R is Tm, Yb, Lu, Mg, Sc, Zr or Hf, crystallize in the $P6/mmm$, number 191, space group. With the exception of $HoFe_6Sn_6$, the space group of the rare-earth RFe_6Sn_6 compounds seems to be determined by the rare-earth size, the smallest crystallizing in the $P6/mmm$ space group and the larger crystallizing in the $Cmcm$ space group. Interestingly, the largest rare earths, such as Pr, Nd and Sm, apparently do not form RFe_6Sn_6 compounds.

Most of the RT_6Sn_6 compounds are antiferromagnetic and only $MgMn_6Sn_6$, $NdMn_6Sn_6$ and $SmMn_6Sn_6$ are ferromagnetic, with Curie temperatures of 290, 357 and 405 K, respectively [5–7]. The rare occurrence of ferromagnetism in the RMn_6Sn_6 compounds is believed to result from the short Mn–Mn distances found in most of the compounds [6], short distances that favour antiferromagnetic interactions.

The substitution of Fe for some of the Mn in the RMn_6Sn_6 compounds generally leads to a decrease in both the Curie temperature and the saturation magnetization. However, unexpectedly, an increase in Curie temperature and saturation magnetization has been observed [6–8] both in $SmMn_{5.5}Fe_{0.5}Sn_6$ and in $NdMn_{6-x}Fe_xSn_6$ when $x \leqslant 2$. X-ray and neutron diffraction studies indicate, at all temperatures studied [8], that $NdMn_6Sn_6$ crystallizes with the $HoFe_6Sn_6$ $Immm$ structure, whereas $NdMn_{6-x}Fe_xSn_6$, with $0.5 \leqslant x \leqslant 2.0$, crystallizes with the $TbFe_6Sn_6$ $Cmcm$ structure. The fractional iron occupancy of the three transition metal sites in the $NdMn_{6-x}Fe_xSn_6$ compounds was obtained [8] from powder neutron diffraction Rietveld refinements. The $NdMn_{6-x}Fe_xSn_6$ compounds exhibit complex magnetic structures with magnetic spin reorientations. In $NdMn_6Sn_6$, the magnetization is perpendicular to the a-axis at 295 K and parallel to this axis below 139 K [8]. In the $NdMn_{6-x}Fe_xSn_6$ compounds, with $x < 2.0$, the magnetic moments make an angle of ca 60° with the a-axis at 295 K and are nearly parallel to the a-axis below their spin reorientation temperatures of 146–260 K. In contrast, in $NdMn_4Fe_2Sn_6$ the magnetic moments are nearly parallel to the a-axis at all temperatures [8].

In order to better understand the role played by the different rare-earth, transition metal and tin sublattices in determining the magnetic properties of the $NdMn_{6-x}Fe_xSn_6$ solid solutions, it is important to independently probe their iron and tin sublattices. In this paper, iron-57 and tin-119 Mössbauer spectral results provide this probe and the results are presented, discussed and contrasted with the previous crystallographic and magnetic results.

2. Experimental details

The $NdMn_{6-x}Fe_xSn_6$ compounds have been prepared as previously described and are the same samples as used in the earlier neutron diffraction and magnetic studies [8].

The iron-57 Mössbauer spectra have been measured at 4.2, 78 and 295 K on a constant-acceleration spectrometer which utilized a room temperature rhodium matrix cobalt-57 source and was calibrated at room temperature with α-iron foil. The Mössbauer spectral absorbers contained 35 mg cm^{-2} of powdered sample which had been sieved to a 0.045 mm or smaller diameter particle size. The iron-57 Mössbauer spectrum of $NdMn_5FeSn_6$ was also measured at 450 K in a locally constructed vacuum oven. The temperature in the oven was measured with an Fe–Rh thermocouple and controlled with an accuracy of ±5 K. The iron-57 spectra have been fitted as explained below and, except as noted in the text, the resulting isomer shifts, quadrupole splittings and line widths are accurate to ca ±0.01 mm s^{-1} and the hyperfine fields to ca ±0.2 T.

The tin-119 Mössbauer spectra have been measured between 85 and 370 K on a constant-acceleration spectrometer which utilized a room temperature $CaSnO_3$ matrix tin-119 source. The spectrometer was calibrated with α-iron and β-tin foils and the isomer shifts are reported

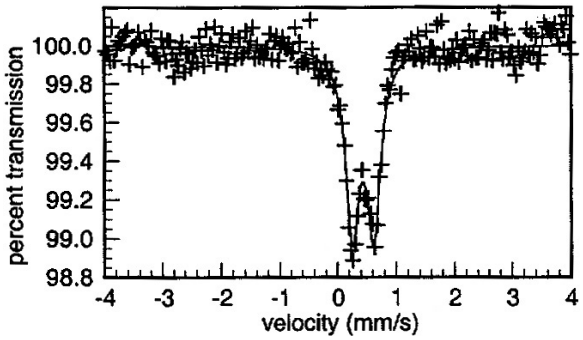

Figure 1. The 450 K iron-57 Mössbauer spectrum of $NdMn_5FeSn_6$.

relative to $CaSnO_3$. The absorbers of $NdMn_{6-x}Fe_xSn_6$ had thickness of ca 25 mg cm^{-2} and were dispersed in boron nitride powder. The tin-119 spectra have been fitted as explained below and the resulting isomer shifts, quadrupole splittings and line widths are accurate to ca ± 0.02 mm s^{-1} and the hyperfine fields to ca ± 0.4 T.

3. Iron-57 Mössbauer spectral measurements

The paramagnetic iron-57 Mössbauer spectrum of $NdMn_5FeSn_6$ obtained at 450 K is shown in figure 1. It has been fitted with one symmetric Lorentzian doublet, with an isomer shift, δ, of 0.434(5) mm s^{-1}, a quadrupole splitting, ΔE_Q, of 0.36(1) mm s^{-1} and a line width, Γ, of 0.29(1) mm s^{-1}. The rather narrow line width, that is only slightly larger than the calibration line width of 0.24 mm s^{-1}, indicates that the three crystallographically distinct iron sites in $NdMn_5FeSn_6$ cannot be resolved and have essentially the same isomer shift and quadrupole splitting at 450 K. Indeed, all three of the iron crystallographic sites in $NdMn_5FeSn_6$ have two neodymium, four manganese or iron and six tin near neighbours and, further, they all have very similar Wigner–Seitz cell volumes. Specifically, the 8d, 8e and 8g Wigner–Seitz cell volumes [8] in $NdMn_{4.5}Fe_{1.5}Sn_6$ are 14.73, 13.27 and 13.05 $Å^3$, respectively, if one uses the 12-coordinate metallic radii of 1.82 Å for Nd, 1.55 Å for Sn and the weighted average of 1.35 Å for Mn and 1.27 Å for Fe. Further, the measured quadrupole splitting is identical to the value of 0.36 mm s^{-1} observed at 600 K [9] in $Yb_{0.6}Fe_6Sn_6$ but is significantly larger than the value of ca 0.27 mm s^{-1} obtained [10] for the RFe_6Ge_6 series of compounds above their ordering temperature.

The iron-57 Mössbauer spectra of the $NdMn_{6-x}Fe_xSn_6$ compounds obtained at 295, 78 and 4.2 K are shown in figures 2, 3 and 4, respectively. The spectra of $NdMn_{6-x}Fe_xSn_6$, with $x = 0.5$ and $x \geqslant 1.0$, have been fitted with two and three sextets, respectively. The relative areas of these sextets have been constrained to the relative iron occupancies of the three crystallographically inequivalent 8d, 8e and 8g sites, as determined [8] from the powder neutron diffraction measurements. Because the three iron sites have the same isomer shift and quadrupole shift in $NdMn_5FeSn_6$ at 450 K, the two or three sextets have been constrained at a given temperature to have the same isomer shift and quadrupole shift but were allowed to have different hyperfine fields. The resulting hyperfine parameters are given in table 1. Alternative fits with three different isomer shift values or with three different quadrupole shift values are not significantly better than those shown in figures 2–4 and no systematic compositional or temperature dependence of the resulting isomer shifts or quadrupole splittings could be observed. Good fits of the spectra of $NdMn_{4.5}Fe_{1.5}Sn_6$ at 78 and 295 K and of $NdMn_4Fe_2Sn_6$

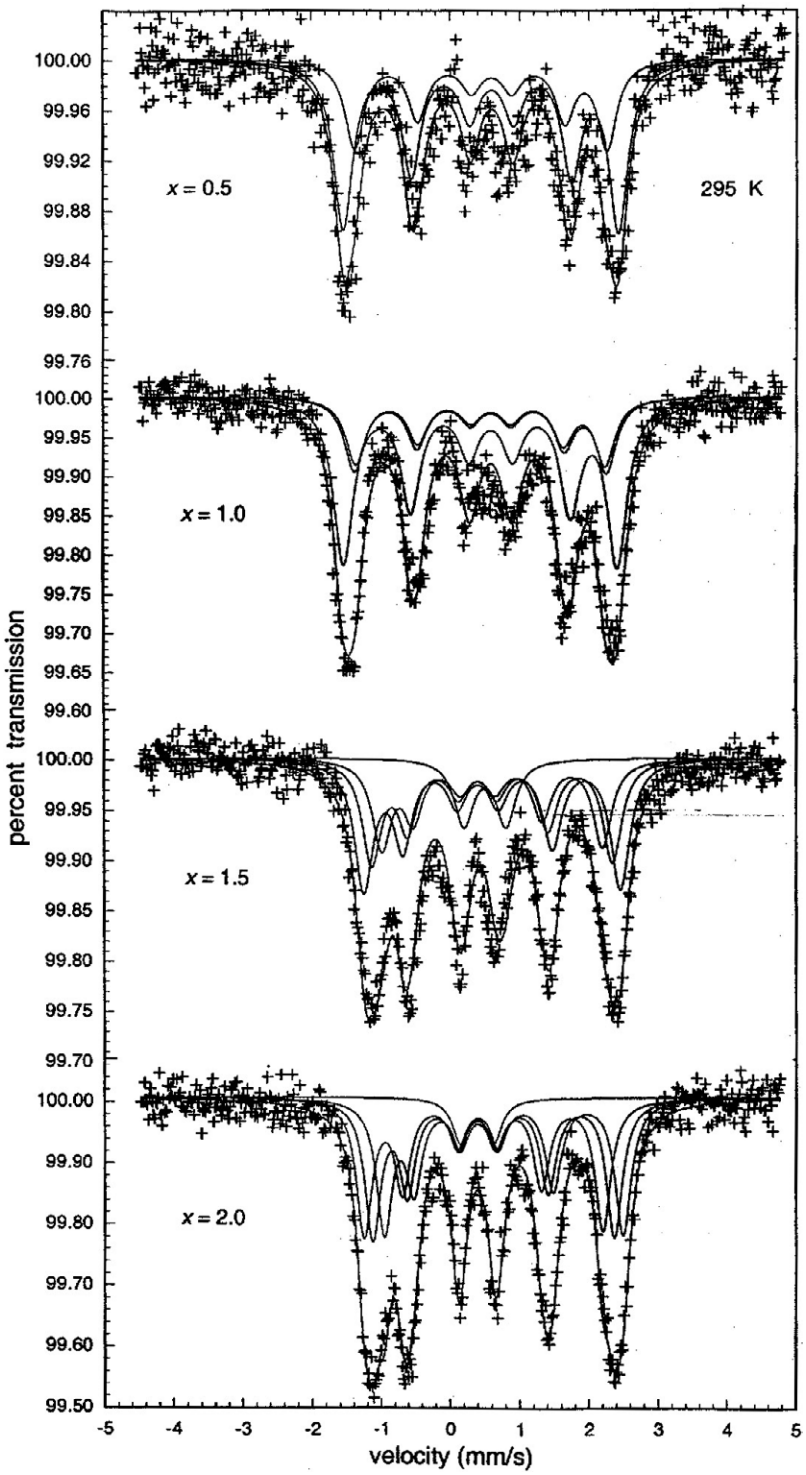

Figure 2. The 295 K iron-57 Mössbauer spectra of the $NdMn_{6-x}Fe_xSn_6$ compounds.

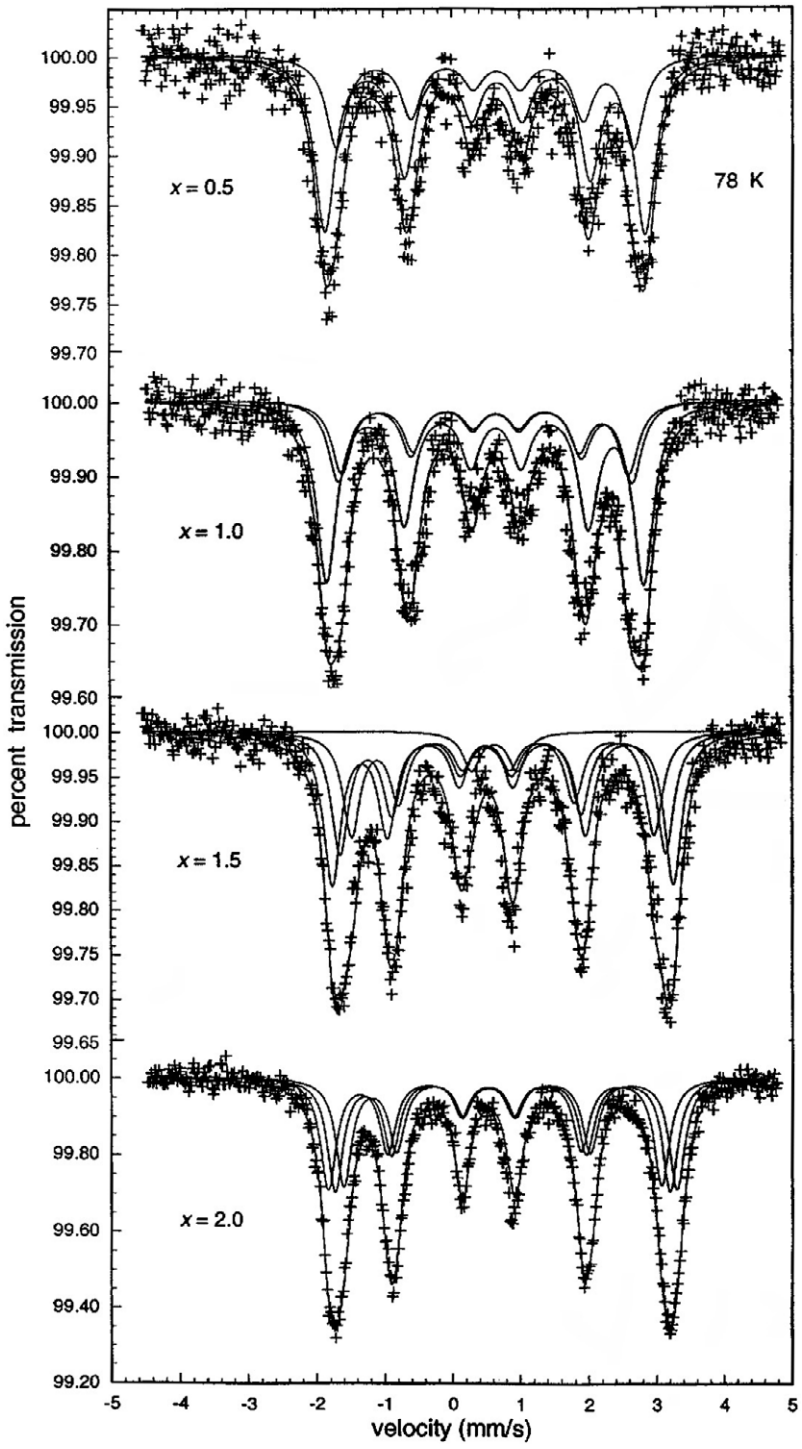

Figure 3. The 78 K iron-57 Mössbauer spectra of the $NdMn_{6-x}Fe_xSn_6$ compounds obtained after slow cooling over approximately one hour from room temperature to 78 K.

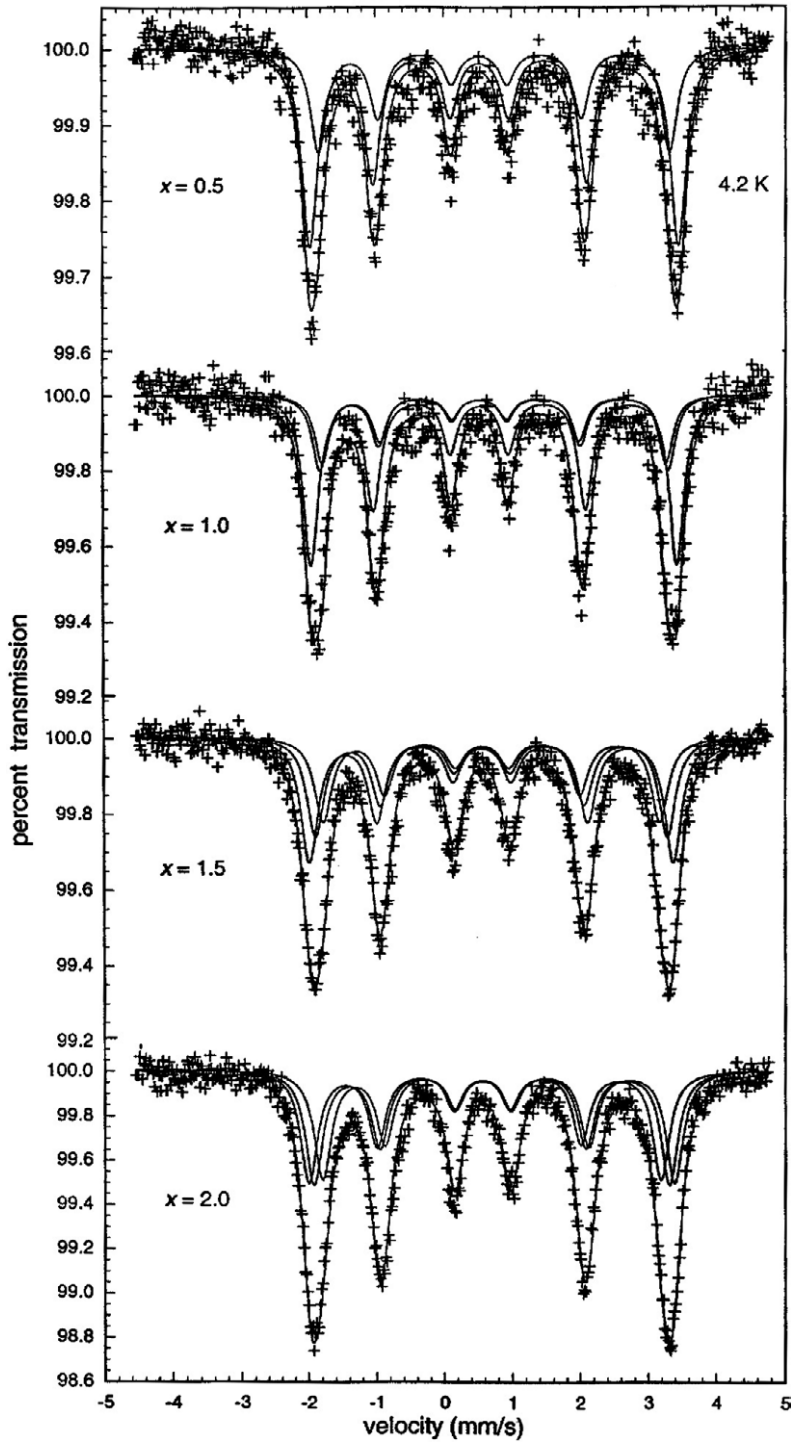

Figure 4. The 4.2 K iron-57 Mössbauer spectra of the $NdMn_{6-x}Fe_xSn_6$ compounds obtained after quenching from room temperature to 78 K and then to 4.2 K.

Table 1. Iron-57 Mössbauer spectral parameters for the $NdMn_{6-x}Fe_xSn_6$ compounds.

x	T (K)	δ [a] (mm s^{-1})	Γ (mm s^{-1})	H_{8e} (T)	H_{8d} (T)	H_{8g} (T)	QS [b] (mm s^{-1})
0.5	295	0.520(4)	0.33(1)	—	11.3(1)	12.35(4)	−0.155(8)
	78	0.580(3)	0.36(1)	—	13.53(8)	14.59(4)	−0.178(6)
	4.2	0.638(2)	0.28(1)	—	15.99(6)	16.80(3)	0.214(5)
1.0	450	0.434(5)	0.29(1)	0	0	0	0.36(1)
	295	0.509(3)	0.35(1)	11.2(5)	11.3(4)	12.28(4)	−0.149(5)
	78	0.570(3)	0.35(1)	13.1(1)	13.4(1)	14.46(3)	−0.160(5)
	4.2	0.635(2)	0.26(1)	15.7(1)	15.9(1)	16.71(3)	0.216(4)
1.5	295	0.508(4)	0.33(1)	9.66(8)	10.82(8)	11.45(7)	0.199(6)
	78	0.616(2)	0.31(1)	13.80(4)	14.88(4)	15.59(3)	0.245(4)
	4.2	0.626(1)	0.30(1)	15.38(4)	16.08(4)	16.63(3)	0.137(3)
2.0	295	0.509(2)	0.28(1)	9.76(3)	10.85(3)	11.64(3)	0.227(4)
	78	0.629(1)	0.28(1)	14.54(3)	15.33(2)	15.96(3)	0.205(2)
	4.2	0.629(1)	0.30(1)	15.49(3)	16.27(4)	16.73(4)	0.131(2)

[a] Relative to room temperature α-iron foil.
[b] QS is the quadrupole shift expressed as $[(6-5)-(2-1)]/2$ except for $x = 1$ at 450 K for which QS is the quadrupole splitting, ΔE_Q.

at 295 K could only be achieved by adding a quadrupole doublet, a doublet which indicates either the presence of an impurity or of a paramagnetic fraction in the sample as a result of sample inhomogeneities. The tin-119 spectra, see below, do reveal the clear presence of an $MnSn_2$ impurity which could, no doubt, contain some iron that would be paramagnetic.

The constraint on the relative areas of the sextets, combined with the observed line shape profile, results in an unambiguous assignment of the three hyperfine fields to the three sites. The 8g site has the largest and the 8e site has the smallest hyperfine field. Further, fits with the alternative field assignments were unacceptable.

The observed iron-57 hyperfine fields in the $NdMn_{6-x}Fe_xSn_6$ compounds are much smaller than the typical hyperfine fields of ca 30 T observed [11, 12] in the ferromagnetic $R_2Fe_{14}B$ and R_2Fe_{17} compounds. The observed hyperfine fields of ca 15 T are even smaller than the 20 T hyperfine fields observed [2, 4, 9, 13] in the RFe_6Sn_6 antiferromagnetic compounds. These small hyperfine fields no doubt result both from the small number, four, of transition metal near neighbours for all the iron sites and from the presence of manganese near neighbours in the environment of the iron, a presence which is expected [14] to further reduce the iron-57 hyperfine field. If the usual proportionality factor of 15 T/μ_B is used, magnetic moments of 1.07–1.11 μ_B per iron are obtained from the 4.2 K hyperfine fields. In terms of the magnetic moment per formula unit, these iron moments, when added to the moment per Mn and Nd obtained [8] for $NdMn_6Sn_6$, yield moments of 17.2, 16.5, 15.8 and 15.1 μ_B per formula unit for the $NdMn_{6-x}Fe_xSn_6$ compounds with $x = 0.5$–2.0, respectively. These values are between the values obtained from the magnetization and neutron diffraction measurements [8]. The same conclusion results even if a conversion factor [16] of only 11.2 ± 2.5 T/μ_B is used in the above calculation.

The 295 K isomer shifts given in table 1 for the $NdMn_{6-x}Fe_xSn_6$ compounds are more positive than the isomer shifts measured [2, 4, 9, 13] in the RFe_6Sn_6 compounds, in agreement [12] with the larger unit-cell volume and, hence, Wigner–Seitz cell volumes in the $NdMn_{6-x}Fe_xSn_6$ compounds. The difference in Wigner–Seitz cell volume for the three sites in $NdMn_{4.5}Fe_{1.5}Sn_6$ is 1.67 Å^3 [8] and does not result in an observable difference in isomer shift. In contrast, in Nd_2Fe_{17}, an increase in Wigner–Seitz cell volume of 0.33 Å^3 upon

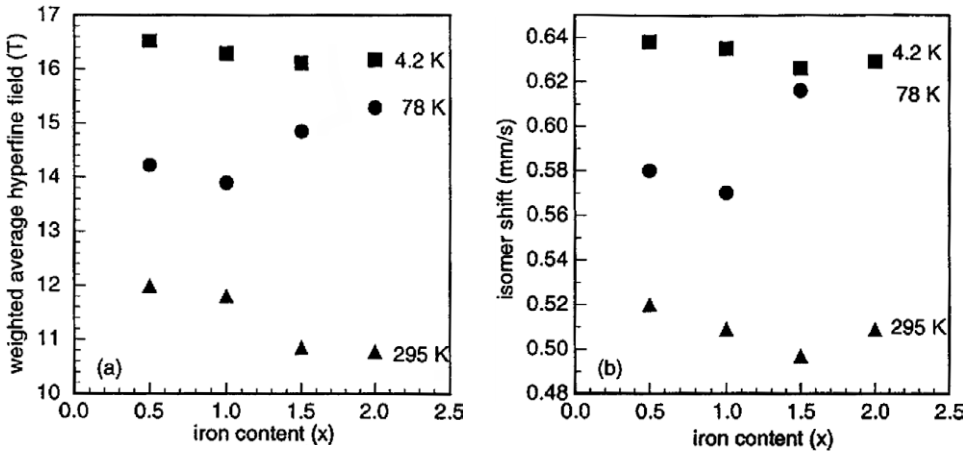

Figure 5. The compositional dependence of the weighted average hyperfine field (a) and of the isomer shift (b) at 4.2, 78 and 295 K. In both plots the error bars are essentially the size of the data points.

nitrogenation leads to an increase in isomer shift of 0.1 mm s^{-1}, an increase which results from the combined effects of the cell expansion and the chemical influence of nitrogen [12]. Further, on the basis of the increases in the average isomer shift and in the average Wigner–Seitz cell volume observed [12] upon nitrogenation of Nd_2Fe_{17}, the average isomer shift for $NdMn_{4.5}Fe_{1.5}Sn_6$ expected from its average Wigner–Seitz cell volume is 0.68 mm s^{-1}, a value which is in good agreement with the observed value of 0.62 mm s^{-1} at 78 K. Hence, the apparently large positive values of the isomer shifts in the $NdMn_{6-x}Fe_xSn_6$ compounds result from the large Wigner–Seitz cell volumes of the iron sites.

The compositional dependence of the weighted average hyperfine field and the isomer shift at 4.2, 78 and 295 K are shown in figures 5(a) and (b). Both parameters show the same behaviour with increasing iron content. At 4.2 K, a temperature at which the four $NdMn_{6-x}Fe_xSn_6$ compounds have the same orientation of their easy magnetization nearly parallel to the a-axis, the weighted average hyperfine field and the isomer shift decrease as the iron content increases, in agreement with the decrease [8] in unit cell volume and iron near neighbour bond distances as the iron content increases. At 295 K, the $NdMn_{6-x}Fe_xSn_6$ compounds, with $0.5 \leqslant x \leqslant 1.5$, have their easy magnetization at an angle of ca 60° from the a-axis and their weighted average hyperfine fields decreases as the iron content increases. At 78 K, the $NdMn_{6-x}Fe_xSn_6$ compounds with $x = 1.5$ and 2.0 exhibit larger weighted average hyperfine fields and isomer shifts than do the $NdMn_{6-x}Fe_xSn_6$ compounds with $x = 0.5$ and 1.0. This different compositional behaviour at 78 K results from the presence of a spin reorientation in the $NdMn_{6-x}Fe_xSn_6$ compounds with $x = 0.5$ and 1.0 between 4.2 and 78 K, a reorientation that will be discussed next in terms of the compositional dependence of the quadrupole shift.

A visual inspection of figures 2–4 reveals the presence of the spin reorientation in some of the $NdMn_{6-x}Fe_xSn_6$ compounds. For $NdMn_{5.5}Fe_{0.5}Sn_6$ and $NdMn_5FeSn_6$ at 295 and 78 K, the spectra show a larger splitting between lines 1 and 2 than between lines 5 and 6, a difference which corresponds to a negative quadrupole shift, QS. In contrast, the spectra obtained at 4.2 K show a smaller splitting between lines 1 and 2 than between lines 5 and 6, a difference which corresponds to a positive quadrupole shift, QS, see figure 6. These changes in sign of the quadrupole shift are a result of changes in the angle, θ, between the principal axis of the

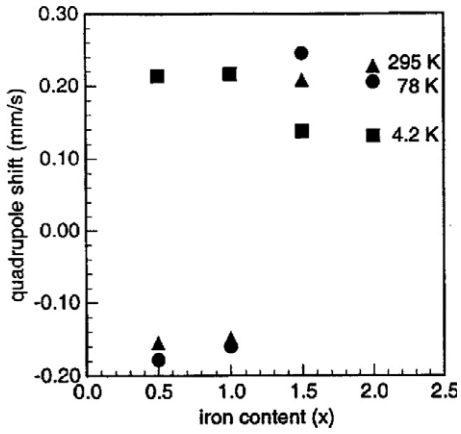

Figure 6. The temperature dependence of the quadrupole shift for the $NdMn_{6-x}Fe_xSn_6$ compounds. The error bars are essentially the size of the data points.

electric field gradient and the hyperfine field; the hyperfine field is assumed to be parallel to the iron magnetic moment. For $NdMn_{4.5}Fe_{1.5}Sn_6$ and $NdMn_4Fe_2Sn_6$, the spectra show a change in the positive value of the quadrupole shift with temperature. Although these changes are without doubt related to a change in the orientation of the iron magnetic moments, they cannot be immediately related to the orientation of the magnetic moments obtained from neutron diffraction. Indeed, it is difficult to determine the direction of the principal axis of the electric field gradient because of the low symmetry of the three crystallographic iron sites and, hence, to obtain the angle, θ, from the known direction of the hyperfine fields which are assumed to be collinear with the iron magnetic moments. However, at this point, one is tempted to conclude that the magnetic structure of $NdMn_{5.5}Fe_{0.5}Sn_6$ and $NdMn_5FeSn_6$ changes between 4.2 and 78 K, whereas $NdMn_{4.5}Fe_{1.5}Sn_6$ and $NdMn_4Fe_2Sn_6$ have the same magnetic structure at the three temperatures. Both of these conclusions disagree with the spin-reorientation temperatures and magnetic moment orientations reported [8] earlier for these samples.

In order to further interpret the changes in quadrupole shift with temperature, the paramagnetic spectrum of $NdMn_5FeSn_6$, shown in figure 1, can be used. Because the sign of the quadrupole splitting, ΔE_Q, is not obtained from the paramagnetic spectrum, both signs must be considered in discussing the relationship between the paramagnetic quadrupole splitting and the magnetic quadrupole shift. However, in the case of $YbFe_6Ge_6$, only the negative sign is compatible [15] with the magnetic spectra. Similarly, negative quadrupole splittings were observed in FeSn [16] and Fe_3Sn_2 [17], compounds that crystallize in structures related to the $TbFe_6Sn_6$ *Cmcm* structure. Finally, the assumption of a positive quadrupole splitting in the discussion below leads to an angle, θ, at 4.2 K which is not in agreement with the orthorhombic structure and leads to values that make the $QS = \Delta E_Q\,(3\cos^2\theta - 1)/2$ equation insoluble at 295 K. Hence, only the negative quadrupole splitting value is considered below.

To a first approximation, we will assume that the asymmetry parameter, η, of the electric field gradient tensor is essentially zero. This approximation may be rather poor as large asymmetry parameters were observed in $YbFe_6Ge_6$ [15], in FeSn [16] and in Fe_3Sn_2 [17]. If we assume that the quadrupole splitting, $\Delta E_Q = e^2Qq/2$, is -0.36 mm s^{-1}, the 4.2 K quadrupole shift, $QS = \Delta E_Q(3\cos^2\theta - 1)/2$, of ca +0.18 mm s^{-1} for the four compounds indicates an angle of 90° between the principal axis of the electric field gradient and the hyperfine field, a field which is parallel to [100]. Hence, the principal axis of the electric field

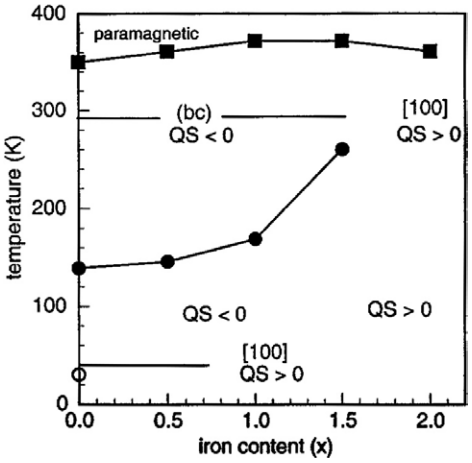

Figure 7. The magnetic phase diagram for the $NdMn_{6-x}Fe_xSn_6$ compounds. The Curie and spin-reorientation temperatures are represented by solid squares and solid circles, respectively. The horizontal lines indicate the temperatures at which the neutron diffraction measurements [8] have been carried out.

gradient lies in the (*bc*) plane. Further, the 295 K quadrupole shift of ca -0.15 mm s^{-1} for $NdMn_{5.5}Fe_{0.5}Sn_6$ and $NdMn_5FeSn_6$ indicates an angle, θ, of 39° between the hyperfine field and the principal axis of the electric field gradient, an axis which lies in the (*bc*) plane. This angle is compatible with the angle, ϕ_a, of ca 60° between the magnetic moments or hyperfine field and the *a*-axis [8]. For instance, if the magnetic moments and hyperfine field are in the (*ac*) plane at an angle of 60° with [100] the principal axis of the electric field gradient may be along [001], or if the magnetic moments and hyperfine field are in the (*ab*) plane at an angle of 60° with [100] the principal axis of the electric field gradient may be along [010]. Unfortunately, as will be discussed below, the negative quadrupole shifts measured at 78 K for $NdMn_{5.5}Fe_{0.5}Sn_6$ and $NdMn_5FeSn_6$ and the positive quadrupole shift measured at 295 K for $NdMn_{4.5}Fe_{1.5}Sn_6$ are not compatible with the neutron diffraction results, presumably because of differing thermal histories for the different measurements.

The changes observed in the line widths given in table 1 also support the change in hyperfine field orientation discussed above. At 4.2 K for all x values and also for $x = 2$ at 78 and 295 K, i.e., for the compounds that have their magnetic moments parallel to [100], a small line width of 0.26–0.30 mm s^{-1} is observed. For $x = 0.5$, 1.0 and 1.5 at 78 and 295 K, i.e., for compounds whose magnetic moments are not parallel to [100], a larger line width of 0.31–0.36 mm s^{-1} is observed. This larger line width reflects the existence of magnetically inequivalent but crystallographically equivalent iron sites in the $NdMn_{6-x}Fe_xSn_6$ compounds, an inequivalence which usually leads [12] to different hyperfine fields as a result of differing orbital and dipolar contributions. In the present case, the hyperfine fields are unusually small and, hence, the difference in hyperfine field between the magnetically inequivalent iron sites is even smaller and is only observed as a broadening [4] of the lines.

The magnetic phase diagram of the $NdMn_{6-x}Fe_xSn_6$ compounds is shown in figure 7. The horizontal lines indicate the two temperatures at which the neutron diffraction measurements have been carried out and are labelled with the direction of the magnetic moments. The observed sign of the quadrupole splitting at 4.2, 78 and 295 K is also indicated. If there is no spin reorientation between 30 and 4.2 K, then a positive quadrupole shift is associated with iron magnetic moments that are nearly parallel to [100]. At 78 K, the compounds with $x = 0.5$

and 1.0 show negative quadrupole shifts, which seem to indicate that they have undergone a spin reorientation between 4.2 and 78 K, whereas magnetization measurements [8] yield spin-reorientation temperatures which are higher than 78 K. The quadrupole shifts for $x = 1.5$ and 2.0 are positive and suggest that the magnetic moments are nearly parallel to [100] at all temperatures, in disagreement and agreement, respectively, with the magnetic and neutron diffraction measurements. The compositional dependence of the weighted average hyperfine field and isomer shift shown in figures 5(a) and (b) also supports the presence of a spin reorientation between 4.2 and 78 K for $x = 0.5$ and 1.0 and its absence for $x = 1.5$ and 2.0.

The difference between the Mössbauer spectral, magnetic and neutron diffraction observations can be reconciled if one assumes that, as is supported by the temperature dependence of the tin-119 Mössbauer spectra to be discussed below, the spin-reorientation transition is very sensitive to slow versus fast cooling, i.e., the $NdMn_{6-x}Fe_xSn_6$ compounds have a history in that they remember whether they have been quenched or slow cooled. The 295 and 78 K spectra have been obtained in the same cryostat on slow cooled samples and do not reveal any spin reorientation on cooling. The 4.2 K spectra have been obtained on samples quenched within one second from 295 to 78 K before being quenched to 4.2 K in liquid helium and, as a consequence, the 4.2 K spectra reveal the spin reorientation. Hence, the iron-57 Mössbauer spectra indicate that the $NdMn_{6-x}Fe_xSn_6$ compounds show a spin reorientation if they are fast cooled but do not show this spin reorientation if they are slow cooled.

4. Tin-119 Mössbauer spectra results

The tin-119 Mössbauer spectra of $NdMn_6Sn_6$ obtained between 85 and 370 K are shown in figures 8(a) and (b). To obtain these spectra the absorber was first slow cooled for ca one hour from 295 to 85 K and then slowly heated over a period of several days from 85 to 370 K. The paramagnetic spectrum obtained above the Curie temperature at 370 K has been fitted with one symmetric quadrupole doublet, with an isomer shift of 1.96 ± 0.01 mm s^{-1} relative to $CaSnO_3$, a quadrupole splitting of 0.97 ± 0.01 mm s^{-1}, and a line width of 1.30 ± 0.01 mm s^{-1}. This broad line mimics the distribution in isomer shifts and/or quadrupole splittings present at the eight crystallographically distinct tin sites in $NdMn_6Sn_6$, eight sites which are not resolved in the 370 K Mössbauer spectrum. Nevertheless, this spectrum yields an upper limit for the quadrupole splitting in $NdMn_6Sn_6$. These tin-119 spectral parameters are similar to those observed [9] for $YbFe_6Sn_6$ in which the three tin sites are characterized at 300 K by a line width of 1.27 mm s^{-1}, an isomer shift of 2.0 mm s^{-1} and a quadrupole splitting of 1.6 mm s^{-1}.

Below the Curie temperature, the spectra in figure 8 exhibit Zeeman split sextets with large transferred hyperfine fields at the eight tin sites. Because tin occupies eight inequivalent crystallographic sites in $NdMn_6Sn_6$, fits of the magnetic spectra with eight sextets with relative area ratio 8:4:4:4:4:4:4:4 have been carried out and are shown in figure 8. The hyperfine parameters obtained from these fits are given in table 2. These fits and the assignment of the eight components to the eight tin sites are based on the Wigner–Seitz cell analysis of these sites.

The Wigner–Seitz cell volumes and the near-neighbour environments of the eight tin sites in $NdMn_6Sn_6$ have been obtained from the 300 K lattice and positional parameters [8] and with the 12-coordinate metallic radii of 1.82, 1.35 and 1.55 Å for neodymium, manganese and tin, respectively, and are given in table 3. The subscripts for the 4g and 4h sites have been given in the sequence used in table 3 of [8]. The eight tin sites are divided into two groups. The first group, consisting of five sites, has the largest Wigner–Seitz cell volumes, the largest total number of near neighbours and at most one neodymium near neighbour. In contrast, the second group, consisting of three sites, has the smallest Wigner–Seitz cell volumes, the smallest total number of near neighbours and two or three neodymium near neighbours. The subspectral

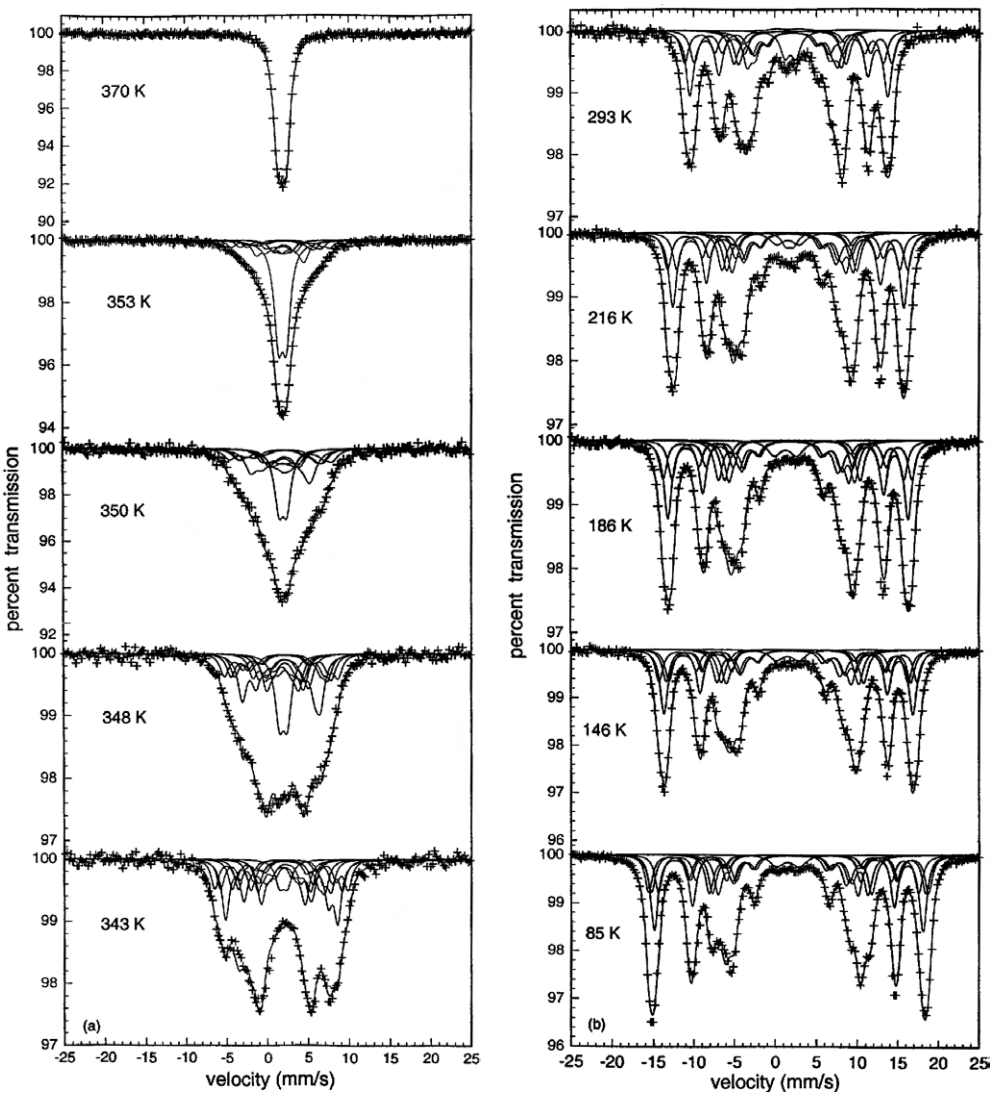

Figure 8. (a) The tin-119 Mössbauer spectra of $NdMn_6Sn_6$ obtained between 343 and 370 K after slowly cooling the absorber for approximately one hour from room temperature to 85 K and subsequently warming over a period of several days. Eight magnetic sextets have been used in each fit, except at 370 K, but in some cases these sextets overlap and are indistinguishable. (b) The tin-119 Mössbauer spectra of $NdMn_6Sn_6$ obtained between 85 and 293 K after slowly cooling the absorber for approximately one hour from room temperature to 85 K and subsequently warming it over a period of several days. Eight magnetic sextets have been used in each fit but in some cases these sextets overlap and are indistinguishable.

components in the 85 K spectrum in figure 8(b) are divided into two groups: first the five sextets with large magnetic fields and relative areas of 8:4:4:4:4, assigned to the 8n, 4e, $4h_2$, $4g_1$ and $4h_3$ sites, and second the three sextets with smaller magnetic fields and relative areas of 4:4:4, assigned to the $4g_2$, $4g_3$ and $4h_1$ sites. The presence of two or three neodymium atoms in the near-neighbour environment of the second group is known [18] to reduce the transferred field on the tin nuclei. The assignment of the sextets to the sites with the same crystallographic

Table 2. Tin-119 hyperfine parameters for $NdMn_6Sn_6$ slowly cooled to 85 K.

Parameter	T (K)	8n	4e	$4h_2$	$4g_1$	$4h_3$	$4g_2$	$4g_3$	$4h_1$
δ [a] (mm s^{-1})	353	1.96	1.96	1.96	1.96	1.96	1.96	1.96	1.96
	350	1.96	1.96	1.96	1.96	1.96	1.96	1.96	1.96
	348	1.96	1.96	1.96	1.96	1.96	1.96	1.96	1.96
	343	1.96	1.96	1.96	1.96	1.96	1.96	1.96	1.96
	293	1.94	1.94	1.85	1.85	1.94	2.34	1.84	1.81
	216	1.93	1.93	1.86	1.86	1.93	2.16	1.82	1.65
	186	1.92	1.92	1.87	1.87	1.92	2.02	1.80	1.80
	146	1.92	1.92	1.89	1.89	1.92	2.06	1.78	1.78
	85	1.91	1.91	1.90	1.90	1.91	2.20	1.84	1.58
	85[b]	1.85	2.2	1.81	2.04	1.90	2.03	2.11	1.92
H (T)	353	4.3	2.5	8.9	7.3	6.1	1.5	1.4	1.4
	350	5.3	3.2	9.3	7.6	7.3	2.5	2.5	1.4
	348	7.0	5.0	10.3	9.1	8.4	3.2	3.9	2.9
	343	10.1	7.8	12.1	11.0	8.9	4.4	5.4	4.2
	293	18.1	17.2	18.9	18.9	17.4	8.9	9.7	9.0
	216	21.2	20.4	22.0	22.0	20.4	11.3	11.8	10.8
	186	22.0	21.2	22.8	22.8	21.2	12.3	11.9	11.3
	146	22.9	22.1	23.7	23.7	22.2	12.9	12.9	11.5
	85	24.7	23.9	25.7	25.7	25.2	14.0	14.5	13.2
	85[b]	28.1	29.5	29.3	27.9	26.3	11.7	10.5	10.4
ΔE_Q [b] (mm s^{-1})	353	0.97	0.97	0.97	0.97	0.97	−0.97	0.97	0.97
	350	1.08	1.08	1.08	1.08	1.08	−1.10	1.20	1.00
	348	1.12	1.12	1.12	1.12	1.12	−0.90	1.00	1.00
	343	1.16	1.16	1.16	1.16	1.16	−1.10	1.20	1.00
	293	1.18	1.18	1.18	1.18	1.18	−1.10	1.22	0.92
	216	1.27	1.27	1.27	1.27	1.27	−0.82	1.07	1.04
	186	1.29	1.29	1.29	1.29	1.29	−0.80	1.10	1.00
	146	1.30	1.30	1.30	1.30	1.30	−0.25	1.00	0.54
	85	1.24	1.24	1.24	1.24	1.24	−0.90	0.86	1.43
	85[c]	0.85	1.36	1.43	1.53	0.98	0.02	0.93	−0.37

[a] The isomer shifts are given relative to room temperature $CaSnO_3$.
[b] An angle, θ, of 90° was fixed for all sites below 353 K.
[c] The absorber has been quenched to 85 K and an angle, θ, of 0° was fixed for all sites.

Table 3. The Wigner–Seitz cell volumes and near-neighbour environments of the tin sites in $NdMn_6Sn_6$.

Sn	8n	4e	$4h_2$	$4g_1$	$4h_3$	$4g_2$	$4g_3$	$4h_1$
V_{WS} (Å^3)	22.74	22.69	22.55	22.37	21.54	21.11	21.04	20.71
n_{total}	14	14	15	15	14	12	13	12
n_{Nd}	1	1	0	0	1	3	2	3
n_{Mn}	6	6	6	6	6	6	6	6
n_{Sn}	7	7	9	9	7	9	8	9

degeneracy of four has been carried out as follows. The isomer shifts of the 8n, 4e and $4h_3$ sites that have identical near-neighbour environment have been constrained to be equal and slightly larger than those of the $4h_2$ and $4g_1$ sites, that also have identical near-neighbour environment. The largest of the three small fields has been assigned to the $4g_3$ site, a site with two neodymium near neighbours. The sextet with the smallest hyperfine field and isomer shift has been assigned to the $4h_1$ site, the site with the smallest Wigner–Seitz cell volume. The

assignment of the 4e and $4h_3$ sites remains tentative. The visible negative quadrupole shift exhibited by the five large field components in the 85 K spectrum is compatible with a positive quadrupole splitting of 1.24 mm s^{-1} and a θ angle of 90° between the hyperfine field and the principal axis of the electric field gradient tensor. An angle of 90° was also used for the $4g_2$, $4g_3$ and $4h_1$ sites and the quadrupole splitting value was fitted. All the fitted quadrupole splitting values at 85 K are compatible with the value of the paramagnetic quadrupole splitting. The spectra between 85 and 350 K were fitted according to the same procedure. Because it is neither easy nor obvious how one can obtain a unique fit of such complex spectra, great care was taken to keep the fitted values of the quadrupole splittings and isomer shifts compatible with the paramagnetic values. Between 343 and 353 K, an additional doublet with hyperfine parameters identical to the paramagnetic doublet was required to obtain a good fit. Its relative area increases as the temperature increases towards the Curie temperature. The temperature dependence of the hyperfine fields both supports the fitting model and suggests the first-order nature of the magnetic transition, as is discussed below.

The 85 K spectrum shown in figure 8(b) is similar to the spectrum of $NdMn_6Sn_6$ obtained at 15 K by Weitzer *et al* [18] but does not show the central peak at ca 0 mm s^{-1}, which is surely due to the presence of some $MnSn_2$ impurity, an impurity which is also observed in the $NdMn_{6-x}Fe_xSn_6$ compounds, as discussed above. Hence, the sample of $NdMn_6Sn_6$ studied herein is closer to a single-phase sample than is the previously studied [18] sample. In spite of this apparent similarity between the 15 K spectrum reported earlier [18] and the 85 K spectrum reported herein, there are subtle differences which are difficult to identify partly because of the small size of figure 2 in [18]. Although the quadrupole shift in the spectrum shown at the top of figure 9 is negative, it is positive in figure 2 of [18]. Further, there also seem to be differences in the line shape profile for lines 3 and 4 in these two figures. These differences result from the different cooling regimes used in cooling the spectral absorber to low temperature. The 85 K tin-119 Mössbauer spectrum of $NdMn_6Sn_6$ obtained after rapid quenching of the absorber from room temperature to 85 K is shown at the bottom of figure 9 and is identical to that of figure 2 in [18]. We are convinced that the spin reorientation at 130 K observed in $NdMn_6Sn_6$ is very sensitive to its rate of cooling. More specifically, we believe that with slow cooling $NdMn_6Sn_6$ will remain in the room-temperature magnetic phase, whereas with fast cooling it undergoes the spin reorientation. Hence, we propose that the spectra in figures 8(a) and (b) and at the top of figure 9 are characteristic of $NdMn_6Sn_6$ with the manganese magnetic moments perpendicular to the [100] direction, whereas the spectrum shown at the bottom of figure 9 is characteristic of manganese magnetic moments along the [100] direction. This sensitivity of the spin reorientation to the rate of cooling was also observed in the $NdMn_{6-x}Fe_xSn_6$ compounds, as was discussed above.

The lower spectrum in figure 9 has been fitted with eight components within the model described above. However, because the hyperfine fields of the five 8n, 4e, $4h_2$, $4g_1$ and $4h_3$ sites are even larger than in the slow cooled spectrum shown at the top of figure 9, different isomer shifts were required to fit these sites. In contrast, the three $4g_2$, $4g_3$ and $4h_1$ sites have smaller hyperfine fields and also require different isomer shifts. These changes in hyperfine field undoubtedly result from a change in the orbital and/or dipolar contributions to the transferred field at the tin nuclei, changes that result from the differing orientation of the manganese and neodymium magnetic moments. Further, the positive observed quadrupole shift in the lower spectrum of figure 9 is compatible with quadrupole splitting values of ca 1.2 mm s^{-1} and a θ angle of 0° between the hyperfine field and the principal axis of the electric field gradient tensor. The fitted quadrupole splitting values are different and in some cases larger than the observed paramagnetic quadrupole splitting, probably as a result of an anisotropic contraction [8] of the unit-cell between 300 and 30 K. The 90° change in the θ angle for the fit of the upper and

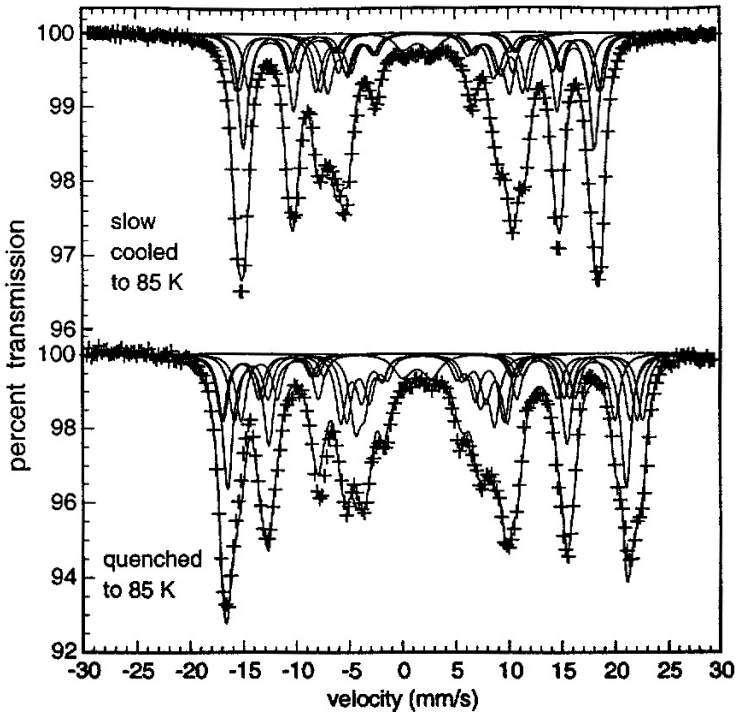

Figure 9. The tin-119 Mössbauer spectra of $NdMn_6Sn_6$ obtained at 85 K after slowly cooling the absorber for approximately one hour from room temperature to 85 K, top, and after quenching the absorber within one second from room temperature to 85 K, bottom. Eight magnetic sextets have been used in each fit but in some cases these sextets overlap and are indistinguishable.

lower spectra shown in figure 9 is the result of the spin reorientation. Because θ is 0° in the lower quenched spectrum, the principal axis of the electric field gradient tensor is parallel to the hyperfine field and magnetic moments and hence is oriented along the [100] or a-axis of the unit cell. In the spectra shown in figure 8 and the top of figure 9, θ is 90°, in agreement with the magnetic moments in the (bc) plane and the orientation of the principal axis of the electric field gradient tensor along the [100] or a-axis of the unit cell.

The reduced weighted average hyperfine field for the 8n, 4e, $4h_2$, $4g_1$ and $4h_3$ sites and for the $4g_2$, $4g_3$ and $4h_1$ sites is plotted as a function of the reduced temperature in figure 10. The reduced fields have been obtained by using extrapolated hyperfine fields at zero temperature of 26 and 14.5 T, respectively, and the reduced temperature has been obtained with a Curie temperature of 355 K. Both reduced fields follow the same temperature dependence and somewhat depart from the solid line that is the Brillouin curve for spin 5/2. The steep decrease in the hyperfine fields above a reduced temperature of 0.8 is indicative of a first-order rather than a second-order transition, in agreement with the magnetostrictive model of Bean and Rodbell [19].

The tin-119 Mössbauer spectra of $NdMn_{5.5}Fe_{0.5}Sn_6$ obtained between 85 and 370 K on a slow cooled sample are shown in figure 11. The spectra have been analysed with five sextets with relative area ratio of 8:4:4:4:4 assigned to the 8g and four 4c sites, in agreement with the crystal structure [8] of the $NdMn_{6-x}Fe_xSn_6$ compounds. Three of the sites, the 8g and two 4c sites, exhibit transferred hyperfine fields of ca 25 T, whereas the other two 4c sites exhibit smaller fields of ca 13 T at 85 K. A tentative assignment of the sextets to the five sites may

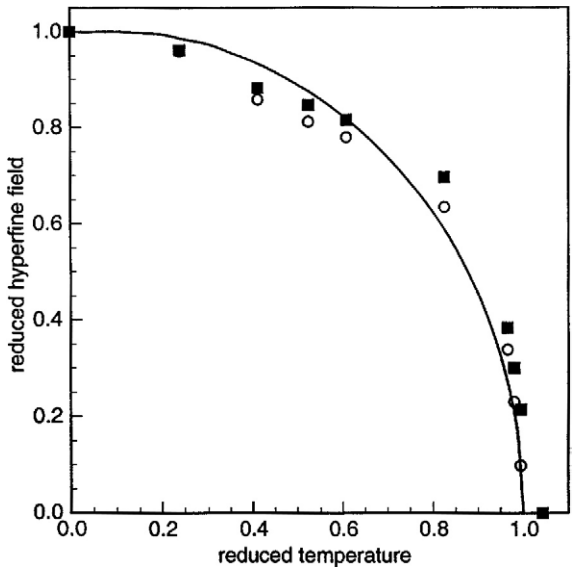

Figure 10. The reduced tin-119 weighted average hyperfine fields for the 8n, 4e, $4h_2$, $4g_1$ and $4h_3$ sites, squares, and for the $4g_2$, $4g_3$ and $4h_1$ sites, circles, in $NdMn_6Sn_6$ as a function of the reduced temperature. The Curie temperature was 355 K and the zero-temperature hyperfine fields have been taken to be 26 and 14.5 T, respectively. The solid line is the Brillouin function for spin 5/2.

be attempted based on the same rationale as was used for $NdMn_6Sn_6$. The Wigner–Seitz cell analysis of $NdMn_{5.5}Fe_{0.5}Sn_6$ indicates that the five tin sites have six Mn/Fe near neighbours, that the $4c_2$ tin site has zero neodymium near neighbours, the 8g and $4c_4$ tin sites have one neodymium near neighbour, the $4c_3$ tin site has two neodymium near neighbours and the $4c_1$ tin site has three neodymium near neighbours. Herein, the 4c sites are numbered 1–4 going down table 4 of [8]. Because the presence of the neodymium near neighbours is known [18] to reduce the transferred hyperfine field, the three large hyperfine fields are assigned to the 8g, $4c_4$ and $4c_2$ sites, whereas the two small fields are assigned to the $4c_1$ and $4c_3$ sites.

The fits shown in figure 11 may not be unique; however, all the tin-119 isomer shifts are reasonable at all temperatures with values ranging from 1.74 to 2.08 mm s^{-1}. The quadrupole splitting values range from −0.50 to 1.80 mm s^{-1} with an angle of 90° between the hyperfine field and the principal axis of the electric field gradient. All these values are similar to those obtained for $NdMn_6Sn_6$. Further, the temperature dependence of the hyperfine fields follows the expected decrease with increasing temperature. Figure 12 shows the reduced weighted average hyperfine field for the two groups of tin sites as a function of the reduced temperature. The reduced fields were calculated with fields of 25 and 13.3 T at saturation and the reduced temperature was obtained from a Curie temperature of 367 K. The reduced fields show a temperature dependence, that is slightly squarer than the Brillouin curve for spin 5/2 shown as a solid line in figure 12. In addition, a reduced plot of the magnetization data above 160 K reported in figure 2 of [8] is typical of a first-order transition with magnetostriction. This behaviour is similar to that observed for $NdMn_6Sn_6$.

The tin-119 Mössbauer spectra of $NdMn_{5.5}Fe_{0.5}Sn_6$ obtained at 85 K on a slow cooled and quenched sample are shown in figure 13 and reveal the same behaviour as observed in $NdMn_6Sn_6$, see figure 9. Hence, $NdMn_{5.5}Fe_{0.5}Sn_6$ shows the same sensitivity of its spin-reorientation transition to its cooling rate. The lower spectrum in figure 13 has also been analysed with five sextets with relative areas of 8:4:4:4:4 and an angle of 0° between the

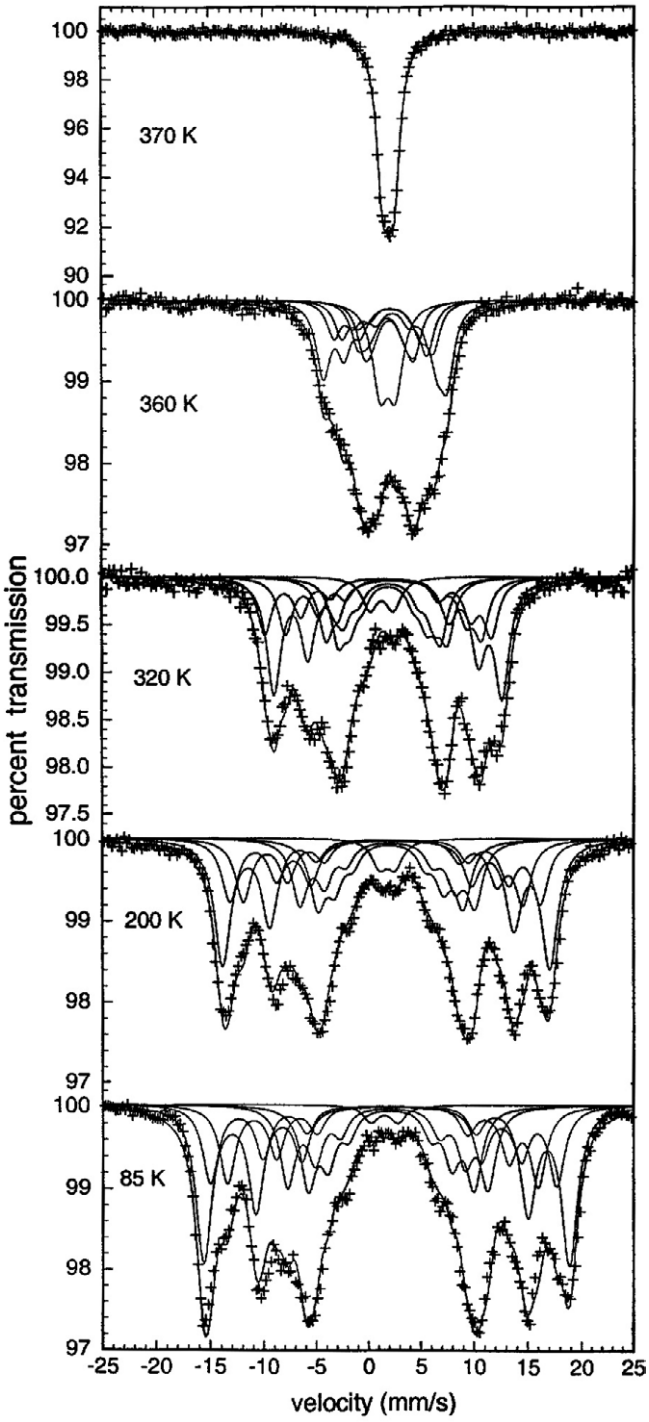

Figure 11. The tin-119 Mössbauer spectra of $NdMn_{5.5}Fe_{0.5}Sn_6$ obtained between 85 and 370 K after slowly cooling the absorber for approximately one hour from room temperature to 85 K and subsequently warming it over a period of several days.

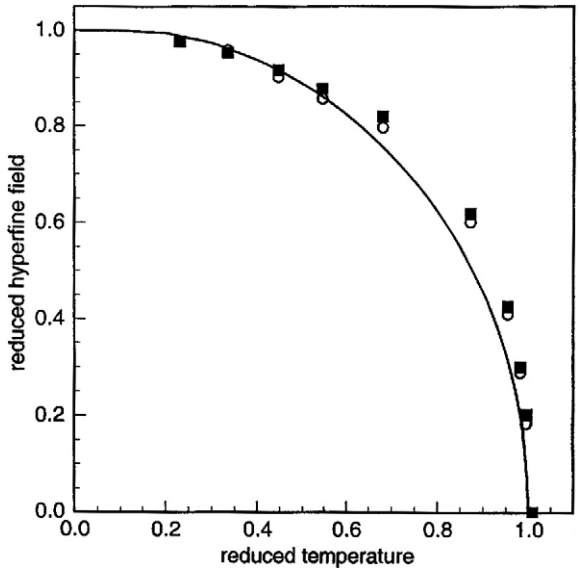

Figure 12. The reduced tin-119 weighted average hyperfine fields for the 8g and two 4c sites, squares, and for the remaining two 4c sites, circles, in $NdMn_{5.5}Fe_{0.5}Sn_6$ as a function of the reduced temperature. The Curie temperature is 367 K and the zero-temperature hyperfine fields have been taken to be 25 and 13.3 T, respectively. The solid line is the Brillouin function for spin 5/2.

hyperfine field and the principal axis of the electric field gradient. The three tin sites with large hyperfine fields exhibit even larger fields, whereas the two tin sites with smaller hyperfine fields exhibit even smaller fields, in a fashion similar to that observed in the spectrum of $NdMn_6Sn_6$ upon quenching.

The tin-119 Mössbauer spectra of the $NdMn_{6-x}Fe_xSn_6$ compounds obtained at 85 K on slowly cooled samples are shown in figure 14. All the spectra have been adequately fitted with five sextets with relative areas of 8:4:4:4:4. However adequate fits could not be obtained with completely reasonable values of the individual isomer shifts and quadrupole splittings. In the fits shown for $x \geqslant 1$ only the average isomer shift and hyperfine field have a physical meaning. The average isomer shift increases with x increasing in disagreement with the decrease in unit cell volume. Hence, the expected volume effect on the isomer shift is overbalanced by a chemical effect of the iron near neighbour of the tin atoms. The 85 K weighted average hyperfine field for the five sites, and the weighted average for the two groups of tin sites in $NdMn_{6-x}Fe_xSn_6$, are plotted as a function of composition in figure 15. The weighted average hyperfine fields decrease linearly with increasing iron content. The 8g, $4c_4$, and $4c_2$ average field decreases by 2.9 T per iron in $NdMn_{6-x}Fe_xSn_6$, whereas the $4c_1$ and $4c_3$ average field decreases by 5.4 T per iron in $NdMn_{6-x}Fe_xSn_6$. The all site average field decreases by 3.7 T per iron in $NdMn_{6-x}Fe_xSn_6$.

Finally, it is clear that the spectra broaden rapidly with an increasing iron content as a result of the distribution of near-neighbour environments around the five tin sites because of the essentially random occupation of the transition metal 8d, 8e and 8g sites.

5. Discussion and conclusions

The combination of iron-57 and tin-119 Mössbauer spectral measurements complements nicely the information gained [8] from neutron diffraction measurements on the $NdMn_{6-x}Fe_xSn_6$

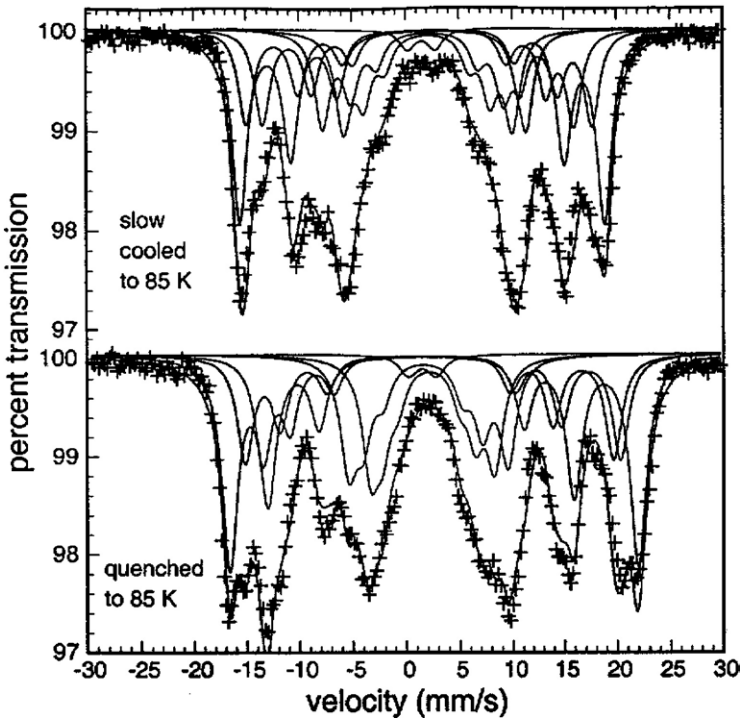

Figure 13. The tin-119 Mössbauer spectra of $NdMn_{5.5}Fe_{0.5}Sn_6$ obtained at 85 K after slowly cooling the absorber for approximately one hour from room temperature to 85 K, top, and after quenching the absorber within one second from room temperature to 85 K, bottom.

compounds. Both series of spectral measurements reveal the sensitivity of the magnetic properties of the $NdMn_{6-x}Fe_xSn_6$ compounds to the rate of cooling of the sample. More specifically, a spin-reorientation transition is observed in both series of spectra if the sample is quenched from room temperature to 78 K, whereas it is not observed if the sample is slowly cooled from room temperature to 78 K. This sensitivity was neither observed earlier [8] in the magnetic measurements nor in the neutron diffraction measurements. The spin reorientation manifests itself in the iron-57 and tin-119 Mössbauer spectra by changes in both the quadrupole shifts and the hyperfine fields observed on the various sites occupied by iron or tin.

The iron-57 hyperfine fields of ca 15 T are unusually small and the tin-119 transferred hyperfine fields of ca 25 T are unusually large. The small iron fields result from the small number, four, of iron or manganese near neighbours. The large tin transferred hyperfine fields are nevertheless smaller than the fields of up to 33 T observed [5] in RMn_6Sn_6, with R = Mg, Zr or Hf. These compounds crystallize with the $HfFe_6Ge_6$ structure, space group $P6/mmm$, a structure which is different from but related to the $HoFe_6Sn_6$ structure, with space group $Immm$, observed for $NdMn_6Sn_6$. Another significant difference between the RMn_6Sn_6 compounds, with R = Mg, Zr or Hf, and $NdMn_6Sn_6$, is the formal trivalent state and magnetic moment of the neodymium. First principles electronic structure calculations [5] on the RMn_6Sn_6 compounds, with R = Mg, Zr or Hf, indicate that the large tin transferred hyperfine fields result from the polarization of the tin valence electrons through the hybridization of the manganese 3d and tin 5s electrons. The average Mn–Sn distances in $NdMn_6Sn_6$ are larger than the average Mn–Sn distances [5] in the RMn_6Sn_6 compounds, with R = Mg, Zr

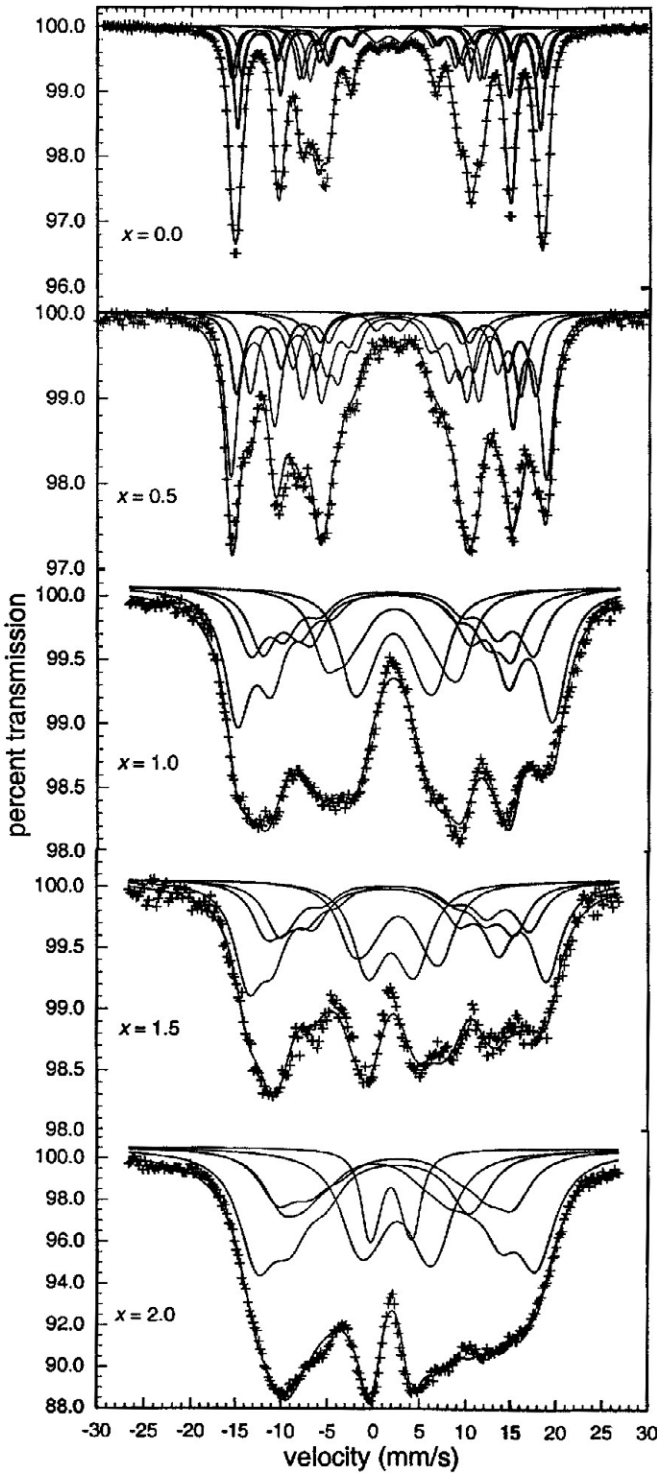

Figure 14. The tin-119 Mössbauer spectra of the $NdMn_{6-x}Fe_xSn_6$ compounds obtained after slowly cooling the absorbers for approximately one hour from room temperature to 85 K.

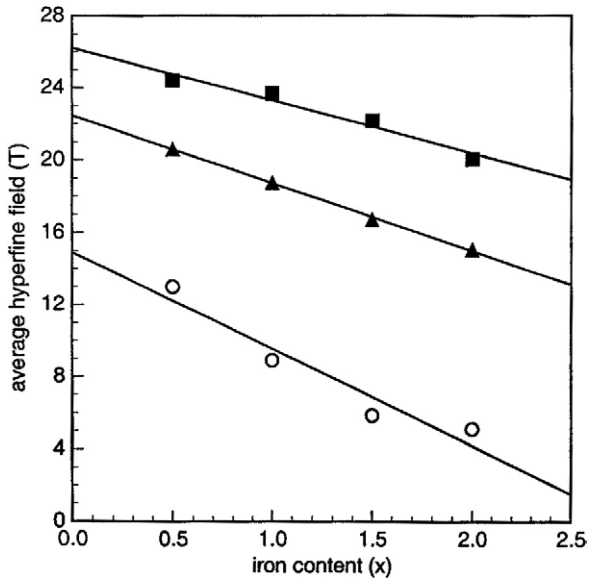

Figure 15. The tin-119 85 K weighted average hyperfine field, triangles, the 8g, $4c_4$, and $4c_2$ weighted average hyperfine field, squares, and the $4c_1$ and $4c_3$ weighted average field, circles, in the $NdMn_{6-x}Fe_xSn_6$ compounds as a function of iron content, x.

or Hf. As a consequence, there is reduction in the Mn–Sn hybridization and thus in the hyperfine fields observed in $NdMn_6Sn_6$. Further, because the neodymium contribution to the tin transferred hyperfine field opposes that of manganese [18], the fields observed in $NdMn_6Sn_6$ are approximately 10 T smaller than those observed in the RMn_6Sn_6 compounds, with R = Mg, Zr or Hf. In both $NdMn_6Sn_6$ and $NdMn_{5.5}Fe_{0.5}Sn_6$ the reduced average transferred hyperfine fields were found to approximately follow a Brillouin curve for spin 5/2. This observation indicates that the major contribution [5] to the transferred field is the Fermi contact field, a field that is proportional to the Mn magnetic moment [8] of ca 2.5 μ_B.

First-principles electronic structure calculations [5] also indicate that the Stoner criterion for ferromagnetism is satisfied in $MgMn_6Sn_6$ because of the presence of a sharp peak in the Mn DOS at the Fermi level. It may reasonably be expected that the same situation occurs in $NdMn_6Sn_6$. When a small amount of iron is introduced into $NdMn_6Sn_6$, some electrons are added in the 3d up band and, as a consequence, both the Curie temperature and the magnetic moment increase, an increase that is in agreement with observation [4]. However, with increasing iron content, the unit cell parameters and the near neighbour distances decrease and favour antiferromagnetic over ferromagnetic interactions. The competition between both effects explains why the improvement in Curie temperature and magnetization is limited to very small iron contents.

Acknowledgments

The authors thank Mr Amitabh Mohan and Ms Leïla Rebbouh for their assistance in obtaining the Mössbauer spectra and Dr J B Yang for his help. The financial support of the National Science Foundation (grant DMR-9614596) and the Defence Advanced Research Projects Agency (grant DAAG 55-98-1-0267) is gratefully acknowledged.

References

[1] Han J, Yelon W B, James W J, Marasinghe G K, Dubenko I and Ali N 2001 *Int. J. Mod. Phys.* B **15** 3223
[2] Cadogan J M, Suharyana, Ryan D H, Moze O and Kockelmann W 2000 *J. Appl. Phys.* **87** 6046
[3] Cadogan J M and Ryan D H 2001 *J. Alloys Compounds* **326** 166
[4] Mazet T and Malaman B 2000 *J. Magn. Magn. Mater.* **219** 33
[5] Mazet T, Tobola J, Venturini G and Malaman B 2002 *Phys. Rev.* B **65** 104406
[6] Marasinghe G K, Han J, James W J, Yelon W B and Ali N 2002 *J. Appl. Phys.* **91** 7863
[7] Malaman B, Venturini G, Chafik El, Idrissi B and Ressouche E 1997 *J. Alloys Compounds* **252** 41
[8] Han J, Marasinghe G K, Yang J B, James W J, Chen M, Yelon W B, L'Héritier Ph, Dubenko I and Ali N 2004 *J. Phys.: Condens. Matter* **16** 5407 (The Wigner–Seitz cell volumes reported herein differ from those reported in table 5 of this paper. Unfortunately, for some unknown reason, we are unable to reproduce the distances and Wigner–Seitz cell volumes given in table 5 from the numbers given in tables 2 and 4.)
[9] Mazet T, Isnard O and Malaman B 2002 *J. Magn. Magn. Mater.* **241** 51
[10] Wang Y B, Wiards D and Ryan D H 1994 *IEEE Trans. Magn.* **30** 4951
[11] Pringle O A, Long G J, Tharp D E, James W J and Yang Y-C 1988 *Hyperfine Interact.* **40** 437
[12] Long G J, Pringle O A, Grandjean F and Buschow K H J 1992 *J. Appl. Phys.* **72** 4845
[13] Rao X L and Coey J M D 1997 *J. Appl. Phys.* **81** 5181
[14] Pringle O A, Fu J, Long G J, James W J, Xie D, Yelon W B and Grandjean F 1990 *J. Appl. Phys.* **67** 4762
[15] Mazet T and Malaman B 2000 *J. Phys.: Condens. Matter* **12** 1085
[16] Häggström L, Ericsson T, Wäppling R and Chandra K 1975 *Phys. Scr.* **11** 47
Häggström L, Ericsson T, Wäppling R and Chandra K 1975 *Phys. Scr.* **11** 55
[17] Le Caër G, Malaman B and Roques B 1978 *J. Phys. F: Met. Phys.* **8** 323
[18] Weitzer F, Leithe-Jasper A, Hiebl K, Rogl P, Qi Q and Coey J M D 1993 *J. Appl. Phys.* **73** 8447
[19] Bean C P and Rodbell D S 1962 *Phys. Rev.* **126** 104